2021-11

Comparative mechanical and microstructural properties of high calcium fly ash one-part geopolymers activated with Na2SiO3-anhydrous and NaAlO2

Wan-En, O

10.1016/j.jmrt.2021.10.018
Journal of Materials Research and Technology
Elsevier

Available online at www.sciencedirect.com

jmr&t Journal of Materials Research and Technology

journal homepage: www.elsevier.com/locate/jmrt

Original Article

Comparative mechanical and microstructural properties of high calcium fly ash one-part geopolymers activated with Na_2SiO_3-anhydrous and $NaAlO_2$

Ooi Wan-En [a,b], Liew Yun-Ming [a,b,*], Heah Cheng-Yong [a,c], Mohd Mustafa Al Bakri Abdullah [a,b], Long-Yuan Li [d], Li Ngee Ho [b], Foo Kai Loong [e], Ong Shee-Ween [a,b], Ng Hui-Teng [a,b], Ng Yong-Sing [a,b], Nur Ain Jaya [a,b]

[a] Geopolymer and Green Technology, Centre of Excellence (CEGeoGTech), Universiti Malaysia Perlis (UniMAP), 01000 Perlis, Malaysia

[b] Faculty of Chemical Engineering Technology, Universiti Malaysia Perlis (UniMAP), 01000 Perlis, Malaysia

[c] Faculty of Mechanical Engineering Technology, Universiti Malaysia Perlis (UniMAP), 01000 Perlis, Malaysia

[d] School of Engineering, Computing and Mathematics, Plymouth University, Drake Circus Plymouth, Devon PL4 8AA, United Kingdom

[e] Institute of Nano Electronic Engineering (INEE), Universiti Malaysia Perlis (UniMAP), 01000 Perlis, Malaysia

ARTICLE INFO

Article history:
Received 24 August 2021
Accepted 4 October 2021
Available online 9 October 2021

Keywords:
One-part geopolymer
High calcium fly ash
Sodium aluminate
Anhydrous sodium metasilicate

ABSTRACT

This paper investigates the effect of varying solid alkali activators on the fresh and hardened properties and microstructural changes of one-part geopolymers (OPGs). Single and binary solid alkali activators were used to activate high calcium fly ash. The alkali activators were either solely sodium metasilicate (Na_2SiO_3) or a combination of sodium aluminate ($NaAlO_2$) and sodium metasilicate (Na_2SiO_3). The OPG activated with anhydrous Na_2SiO_3 achieved an excellent 28-day compressive strength of 83.6 MPa while OPG activated with $NaAlO_2$ and Na_2SiO_3 attained a compressive strength of 45.1 MPa. The Na_2SiO_3-activated OPG demonstrated better fluidity than the OPG activated with $NaAlO_2$ and Na_2SiO_3 due to the thixotropic behaviour caused by the $NaAlO_2$. The Na_2SiO_3-activated OPG consisted of sodium-calcium aluminium silicate hydrate ((N,C)-A-S-H) gel phase, while the OPG activated with $NaAlO_2$ and Na_2SiO_3 comprised of the coexistence of sodium aluminium silicate hydrate (N-A-S-H) and calcium aluminium silicate hydrate (C-A-S-H) gel phases. Regardless of the distinctive properties, the OPGs are adequate for building materials applications.

* Corresponding author.
E-mail address: ymliew@unimap.edu.my (L. Yun-Ming).

https://doi.org/10.1016/j.jmrt.2021.10.018

1. Introduction

Ordinary Portland Cement (OPC) is a binder material in concrete that has monopolized the construction and building industry for decades. The manufacturing of OPC requires the exploitation of natural resource, such as limestone, and high energy consumption from the calcination of the limestone [1]. The chemical reaction involved in the manufacturing process of OPC contributes to approximately 8% of the global CO_2 emission, which has been rated as the world's third-largest source of CO_2 emission [2]. The rising awareness on global warming, increases the demand for environmentally friendly materials to substitute the polluting materials, especially OPC. Amongst all, the introduction of one-part geopolymer (OPG) is one of the approaches to resolve the depressing issue. According to Luukkonen et al. [1], the environmental impact of OPG is only 24% of the environmental impact contributed by OPC. Therefore, OPG currently thrives in the field of construction materials.

The evolution of OPG has been adapted from the geopolymerisation reaction, where the resulting product is an inorganic binder with sialate networks consists of silicate (SiO_4) and aluminate (AlO_4) tetrahedrally linked by sharing all the oxygens [3]. OPG can be produced by mixing aluminate- and silicate-containing material with solid alkali activator in the presence of water. The reactive aluminosilicate precursor can be industrial waste materials, such as fly ash, slag and rice husk ash, whereas the solid alkali activator can be alkali hydroxide, silicate, aluminates, carbonates, sulphates, or a blend of these materials [4]. The chemistry involved after the addition of water into the dry binder are ion exchange, hydrolysis, network breakdown, and the release of Si and Al [5]. The "just add water" approach makes up for the shortcomings of the traditional two-part geopolymer. The fabrication process of traditional two-part geopolymer involves the transportation, storage and handling of hazardous activating solutions, which significantly reduced the commercial potential of this material. On the contrary, the simple and safe processing route of OPG fabrication has drawn the attention of researchers in recent years.

Raw material selection is a key feature that determines the behaviour of fresh and hardened properties of the resulting OPG due to the distinctive reaction between the elements. Fly ash is categorised into Class F and Class C as accordance to ASTM C618-19 based on the calcium oxide (CaO) content. Class F fly ash has CaO content lower than 18% while the Class C fly ash has CaO content greater than 18.0%. Most studies focused on using the blend of Class F fly ash and blast furnace slag [6–9]. This is because the higher calcium content in slag favours the formation of calcium aluminium silicate hydrate (C-A-S-H) gel in addition to the sodium aluminium silicate hydrate (N-A-S-H) gel, which is the conclusive factor of compressive strength [6,10]. In return, fly ash and slag-blend OPG demonstrate higher mechanical properties compared to single fly ash-based OPG. For example, the 7-day compressive strength of fly ash-based geopolymer was 3 MPa, while a substitution of 20% slag in the OPG increased the compressive strength to 40 MPa based on Oderji et al. [7]. However, the study also pointed out that the angular slag particles deteriorated the workability of the OPG slurries. One of the methods to reduce the incorporation of extra precursors for OPG while maintaining the strength is to apply fly ash with a higher CaO content. Mohammed et al. [11] reported a compressive strength of 50 MPa with excellent flowability for OPGs synthesised with high calcium fly ash and anhydrous-Na_2SiO_3. Nonetheless, the pore content and the effect of water content in the one-part mixtures are not studied. The porosity of the OPG structure is essential to support the mechanical properties and envisage the durability performances. The behaviour of OPG slurries with varying water content is a vital application knowledge. According to Ma et al. [6], Na_2SiO_3-anhydrous is the most suitable activator for preparing OPGs in comparison to other commercial sodium metasilicates. However, Na_2SiO_3-anhydrous is expensive and the production process releases a huge amount of CO_2 with an average CO_2 equivalent (CO_2-e) emission of 1.86. Thus, other lower-cost alkaline materials should be considered to completely replace, or at least partially substitute anhydrous Na_2SiO_3 in the synthesis of OPG.

Solid sodium aluminate ($NaAlO_2$) is readily dissolved in water [12], which makes it a potential solid alkali activator for OPG. Hajimohammadi and Deventer [13] discovered that the aluminate source dissolved faster at the early stages of geopolymerisation reaction, but contributed to slower geopolymer formation. The driving force of Al removal from the precursor was reduced under Al-rich conditions, leading to a lower dissolution rate of the precursor, and thus, a slower formation of geopolymer gel. A high degree of reaction was reported by Sturm et al. [14] for the $NaAlO_2$-activated rice husk ash OPG. However, the strength gain of the OPG was inauspicious. The compressive strength dropped from 32.7 to 30.1 MPa (from day 3 to day 7). The finding suggests that other potential precursor materials could be mixed with solid $NaAlO_2$ to enhance the strength development of the OPG. The solid $NaAlO_2$ is mostly being treated as the aluminate source to pair with silica-rich precursors, such as geothermal silica [13], rice husk ash [12,14] and microsilica [15,16]. These studies focus mainly on the degree of reaction and material characterization. The fresh and physical properties which are the indispensable aspects to certify the practicability in application are not focused on their research.

One-part geopolymer based on Class F fly ash and metakaolin with slag incorporation has been widely reported. However, the one-part geopolymer based on solely Class C fly ash is very little. In addition, the use of sodium silicate in synthesis of one-part geopolymer is common. This study proposes the use of sodium aluminate to replace portion of sodium silicate in the synthesis of one-part geopolymer, which is less reported, especially for one-part geopolymer based on Class C fly ash. Therefore, in this study, two OPG systems were developed: the OPG M system with single alkali activator (that is, anhydrous Na_2SiO_3) and the OPG MA system with binary solid alkali activators (that are, solid $NaAlO_2$ and Na_2SiO_3). This paper compares and elucidates the difference in the one-part geopolymer systems fabricated using different solid activators. The materials properties of the one-part geopolymer has been comprehensively discussed in this paper.

Table 1 – Chemical compositions of fly ash determined by X-ray Fluorescence (XRF) analysis.

Component	SiO_2	Al_2O_3	Fe_2O_3	CaO	SO_3	K_2O	TiO_2
Fly ash (%)	36.7	18.7	17.2	19.1	3.04	1.78	1.68

2. Experimental work

2.1. Materials

The fly ash used in this study was Class C fly ash in accordance with ASTM C618-19. It was obtained from Sultan Azlan Shah Power Plant in Sri Manjung, Perak, Malaysia. The oxides compositions of the fly ash that were determined using X-ray fluorescence (XRF) analysis are displayed in Table 1. The major oxides present in the fly ash were silica, alumina and calcium oxide. The particle size distribution of fly ash is shown in Fig. 1. The fly ash had 58% of particles finer than 10 μm, with d(0.1) of 1.0 μm, d(0.5) of 7.8 μm, and d(0.9) of 29.5 μm. The SEM image of the fine spherical fly ash is displayed in Fig. 2.

The fly ash was activated with anhydrous sodium metasilicate (Na_2SiO_3) and sodium aluminate ($NaAlO_2$). The anhydrous Na_2SiO_3 (Alfa Aesar) was supplied by Fisher Scientific (M) Sdn. Bhd. It was in granular form (18-mesh), consisting of 44.7%–47.6% of SiO_2 and 49.1%–51.7% of Na_2O. The $NaAlO_2$ powder (Sigma–Aldrich) contained 50.0%–56.0% of Al_2O_3 and 37.0%–45.0% of Na_2O.

2.2. Preparation of one-part geopolymer (OPG)

Two OPG systems were prepared with a respective range of mixing compositions. Table 2 lists the details of mixture and the corresponding weight of the respective raw materials. The M system contained only anhydrous Na_2SiO_3 as the sole alkali activator, while the MA system consisted of both anhydrous Na_2SiO_3 and $NaAlO_2$ as the solid alkali activators. The alkali activator-to-fly ash (AA/FA) ratio was defined as the weight ratio of the solid alkali activators (Na_2SiO_3 or Na_2SiO_3 + $NaAlO_2$) to fly ash. The water-to-binder (W/B) ratio indicated the weight ratio of water to dry binder (solid alkali activator(s) + fly ash). An additional manipulative factor, that was the sodium aluminate-to-sodium metasilicate ($NaAlO_2$/Na_2SiO_3) weight ratio was examined for OPG MA system. The mix compositions were referred from preliminary tests and previous research work in this area of study [10,17].

All raw materials were weighed according to the mix design and dry-mixed for one minute. Then, water was gradually added into the mixture and mechanically mixed for three minutes to produce a geopolymer slurry. Upon completion of the mixing process, the slurry was rapidly casted into 50-mm cubic moulds in accordance with ASTM C109/C109M-13. The first pour depth was set to about one-half of the mould depth (approximately 25 mm) and was tamped 32 times before the second layer was poured in and compacted again. After moulding, the samples were vibrated using vibrating table for one minute followed by all-round wrapping using a cling film to prevent moisture loss during the ageing process. The samples were demoulded after being stored at room temperature (30 °C) for 24 h. The samples were aged for 28 days before testing and analysis.

2.3. Testing procedure

The fresh properties of the OPG mixes evaluated were fluidity and setting time. Fluidity was tested based on the guideline provided in the BS EN445. The fluidity test used a cylindrical plastic tube and a smooth glass plate (as shown in Fig. 3). The tube was first placed at the centre of the plate and filled up with freshly mixed OPG paste. The filled mould was then lifted vertically above the base plate to allow fresh slurry to spread. The spread dimension of the paste was measured in two perpendicular directions after 30 s of lifting. The fluidity was the calculated value of the average diameter of the spread.

To determine the setting time of the OPG mixtures, the Vicat setting time testing modified from ASTM C191-08 was

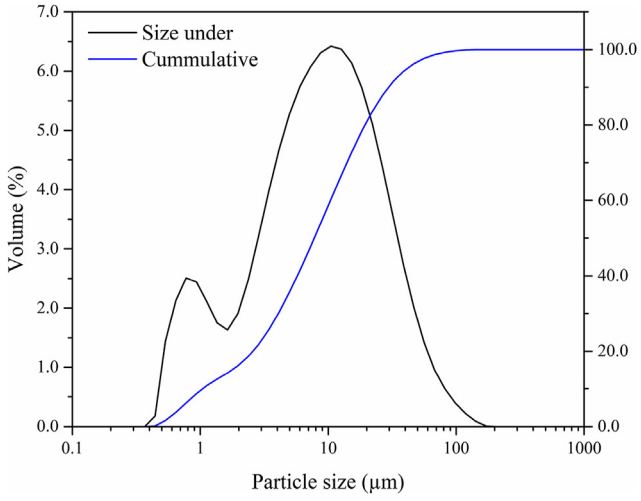

Fig. 1 – Particle size distribution and cumulative particle size of fly ash.

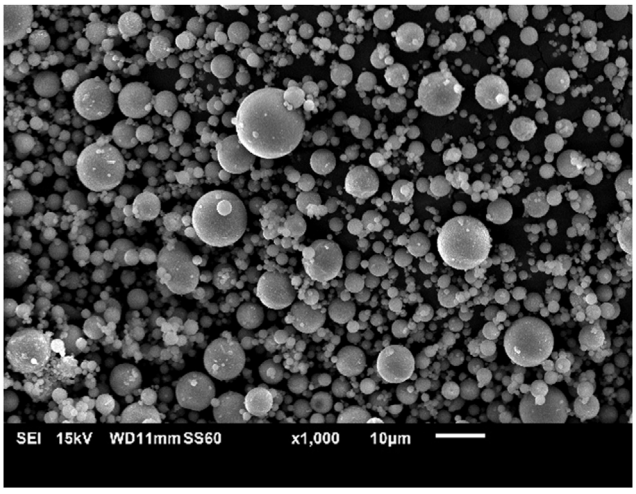

Fig. 2 – SEM image of fly ash (magnification 1000×).

Table 2 – Details of mixture of OPGs.

Binder name	AA/FA ratio	$NaAlO_2/Na_2SiO_3$ ratio	W/B ratio	Quantity of material for 125 cm^3			
				Fly ash (g)	Na_2SiO_3 (g)	$NaAlO_2$ (g)	Water (g)
M1	0.10	–	0.25	181.82	18.18	–	50.00
M2	0.15	–	0.25	173.91	26.09	–	50.00
M3	0.20	–	0.25	166.67	33.33	–	50.00
M4	0.25	–	0.25	160.00	40.00	–	50.00
M5	0.20	–	0.20	173.61	34.72	–	41.67
M6	0.20	–	0.25	166.67	33.33	–	50.00
M7	0.20	–	0.30	160.26	32.05	–	57.69
MA1	0.10	1.50	0.40	162.34	6.49	9.74	71.43
MA2	0.15	1.50	0.40	155.28	9.32	13.98	71.43
MA3	0.20	1.50	0.40	148.81	11.90	17.86	71.43
MA4	0.25	1.50	0.40	142.86	14.29	21.43	71.43
MA5	0.20	1.50	0.40	148.81	11.90	17.86	71.43
MA6	0.20	2.00	0.40	148.81	9.92	19.84	71.43
MA7	0.20	2.50	0.40	148.81	8.50	21.26	71.43
MA8	0.20	3.00	0.40	148.81	7.44	22.32	71.43
MA9	0.20	2.50	0.35	154.32	8.82	22.05	64.81
MA10	0.20	2.50	0.40	148.81	8.50	21.26	71.43
MA11	0.20	2.50	0.45	143.68	8.21	20.53	77.59

adapted. The OPG slurry was compacted into a ring mould, then left to set for 15 min before commencing the measurement. A 1-mm thick Vicat needle was positioned right above the geopolymer paste and the indicator was set to zero. The movable rod was released at an interval of 15 min. The time when the penetration was less than 25 mm was recorded as the initial setting time, whereas the final setting time was logged when the Vicat needle did not mark the specimen surface with a complete circular impression.

After 28 days of ageing, the cube specimens were collected for physical analysis. The bulk density of OPG was measured in accordance with BS EN 12390-7, by using the mass of the specimen divided by its volume. The water absorption and porosity of OPG was determined in accordance with ASTM C642-13. This testing involved the Archimedes principles. The samples were first dried in an oven at a temperature of 80 °C for 24 h and the weight of oven-dried samples were recorded as M_D. The dried samples were tied up using thin wire and fully submerged into tap water. The weight of the suspended samples was recorded as M_S. Next, the samples were immersed in water for 24 h. The wet samples were weighed and recorded as M_W. The water absorption ability and pore content of the samples were calculated using Equations (1) and (2), respectively.

$$\text{Water absorption}(\%) = \frac{M_W - M_D}{M_D} \times 100 \quad (1)$$

$$\text{Porosity}\ (\%) = \frac{M_W - M_D}{M_W - M_S} \times 100 \quad (2)$$

Compressive test of hardened OPG specimens were executed in accordance with ASTM C109/C109M-13. The compressive test was carried out using a Universal Testing Machine (UTM) modelled Shimadzu UH-1000kNI with a constant loading placement rate of 5 mm/min. Data were collected from 3 samples for every set of geopolymer mixture to obtain the average strength value.

Images for microstructural analysis were obtained using a scanning electron microscopy (SEM) modelled JEOL JSM-6010LV. OPG specimens for microstructural analysis were

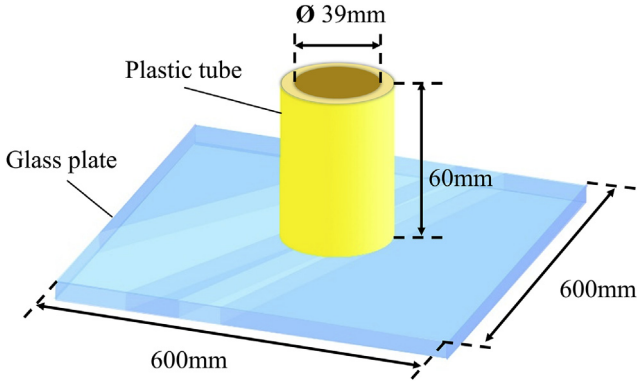

Fig. 3 – Apparatus set up for fluidity test.

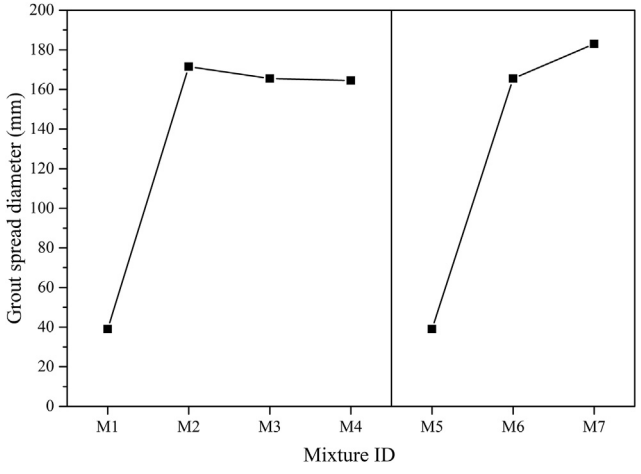

Fig. 4 – Grout spread diameter of OPG M system.

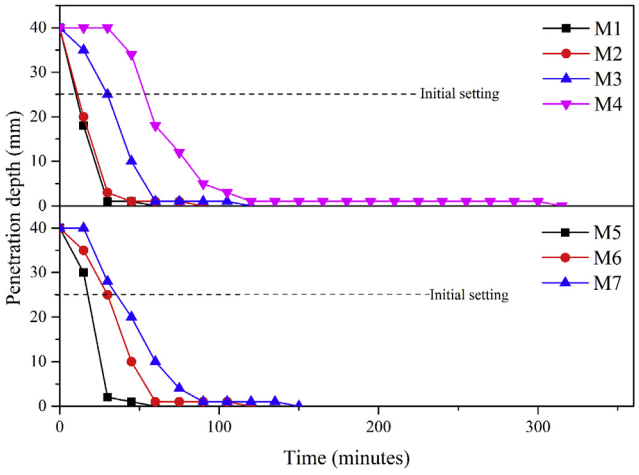

Fig. 5 – Vicat setting time of OPG M system.

prepared separately to prevent unnecessary cracks formation on the SEM specimens. The phases present in the fly ash and optimised OPG were identified through using the D2-Phaser Bruker X-ray diffractometer with Cu-kα radiation. The analysis on powdered specimens was conducted with the scan degree ranging from 10° to 80° and scan rate of 1.0 s/step. The diffraction pattern was analysed using X'Pert HighScore Plus software. Functional groups present in fly ash and the OPG were identified using the PerkinElmer Spectrum RX1 Fourier transform infrared (FTIR) spectroscopy. The powdered specimens were scanned from 650 cm^{-1} to 4000 cm^{-1} with a resolution of 4 cm^{-1}.

3. Results and discussion

3.1. *One-part geopolymers with anhydrous Na_2SiO_3 (M system)*

3.1.1. *Fluidity*

Fig. 4 displays the grout spread diameters of the fresh paste of OPG M system with varying AA/FA and W/B ratios. Note that the fresh OPG paste with larger spread diameter indicates mixture with less viscosity and better fluidity. The fluidity was poor at AA/FA ratio of 0.10 (M1), but it was enhanced when slightly more alkali activator was added. The fluidity of OPG was influenced by the dissolution of solid alkali activator after the addition of water. Extensive dissolution and disaggregation of the raw materials reduced the resistance between the solid particles and promoted better dispersion of the elements in the pastes, thus, better fluidity could be achieved. The M1 paste with low alkali content experienced poor alkaline hydrolysis, yielding binder with high resistance and poor fluidity. The great difference in fluidity with small variances of AA/FA ratio from AA/FA ratio 0.10 (M1) to 0.15 (M2) demonstrated the sensitivity of fly ash towards the pH of the mixture.

When the AA/FA ratio was increased from 0.15 (M2) to 0.25 (M4), a reduction of spread diameter from 172 to 165 mm was observed. A similar trend was reported by Yang et al. [18] whereby the addition of sodium silicate content resulted in

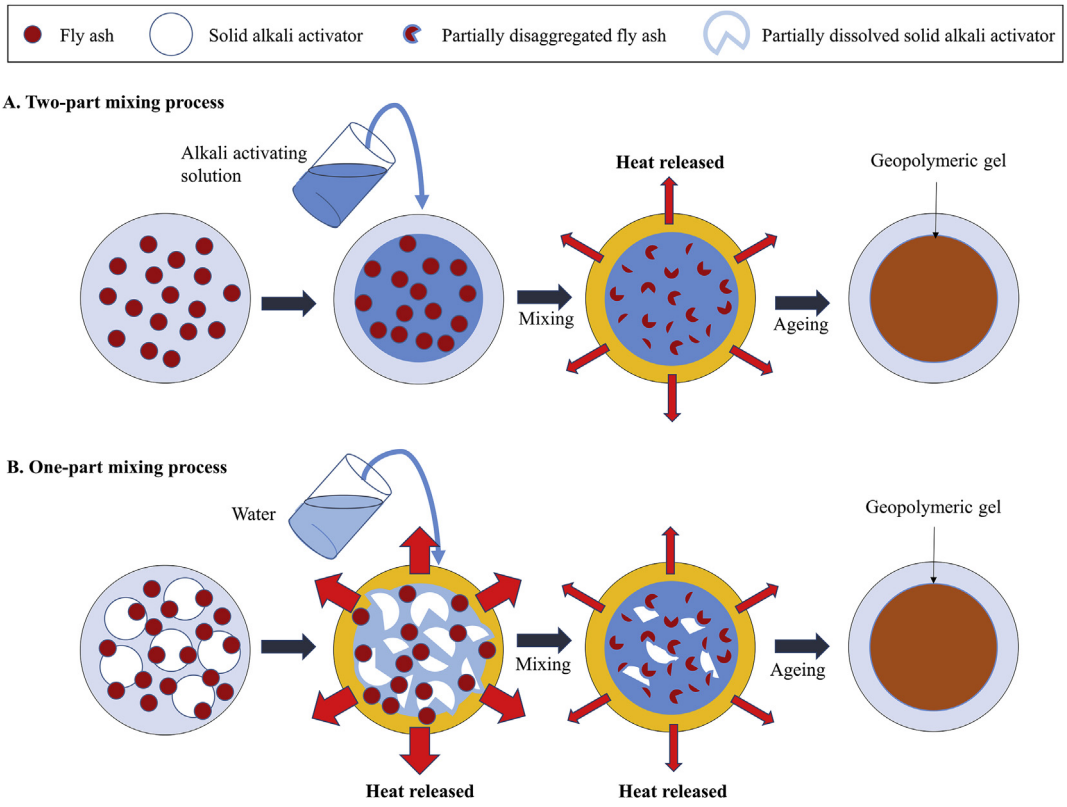

Fig. 6 – Schematic diagram of the mixing process of traditional two-part geopolymer and OPG.

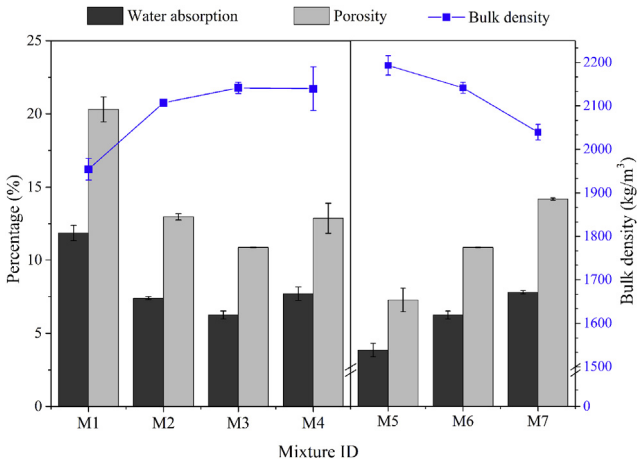

Fig. 7 – Bulk density, water absorption and porosity of OPG M system.

lower initial flow. It is important to note that the Na_2O compound is viscous. Increasing AA/FA ratio delivers a mixture with a higher concentration of Na_2O, thus reduces the fluidity. Furthermore, when the concentration of Na_2O and SiO_2 compounds in a mixture is high, further dissolution of the Na_2SiO_3 coarse granules is restricted. High sliding friction occurs and reduces the spread diameter. Thus, the OPG paste becomes stiffer when the AA/FA ratio is increased. This phenomenon is similar to the traditional geopolymer as the workability of traditional two-part mixing geopolymer relies on the viscosity of the alkali activating solution. The viscosity increases along with the concentration of Na_2SiO_3 solution [19].

The fluidity of OPG paste was enhanced with the increase of the W/B ratio. The spread diameter increased by 144 mm when the W/B ratio was increased, at a constant AA/FA ratio. This was likely due to the higher liquid and lesser solid fraction that attributed more liquefied slurries, eventually enhanced the mobility of elements in the mixture. Note that the spread diameters of M1 and M5 slurries were 39 mm, which were the same as the inner diameter of the cylinder tube (Fig. 3). These slurries had a low fluidity and were not favourable for application.

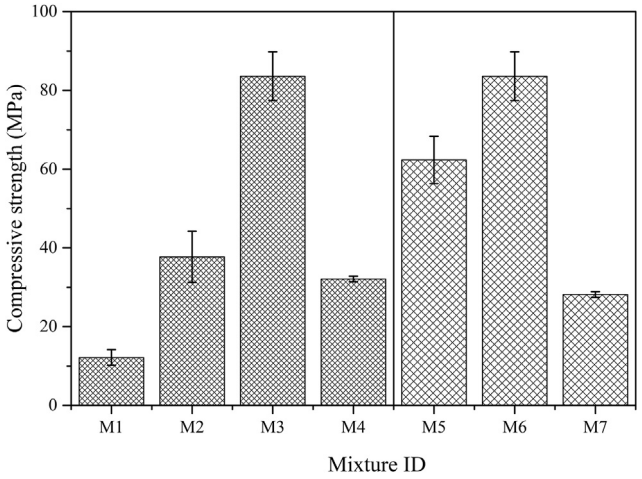

Fig. 8 – Compressive strength of OPG M system.

3.1.2. *Setting time*

Fig. 5 shows that increasing the AA/FA ratio and W/B ratio of the OPG M system had prolonged the rate of geopolymerisation reaction. The initial setting time of M1 to M4 retarded from 10 to 55 min, while the final setting time increased from 60 to 315 min. The increase of Na_2SiO_3 with increasing AA/FA ratio was equivalent to the increase of silicate amount. The delayed setting time was due to the slower condensation between silicate species in comparison to the condensation between silicate and aluminate [20]. Furthermore, the restricted mobility within the slurries due to decreased fluidity at a higher AA/FA ratio also contributes to the delayed rearrangement of gels. Consequently, a longer time was required for the build-up of interconnecting geopolymeric networks. Although increasing the water content of the mixtures allowed better mobility, the setting time was not shortened as high amount of water has to be released during the coagulation and condensation process.

The geopolymerisation reaction of OPG could only be commenced with the addition of water when there is sufficient dissolution of solid alkali activators or adequately high pH conditions to promote disaggregation of fly ash particles. Therefore, the setting time of OPG are expected to be longer than that of traditional geopolymer as more time is required to cultivate a suitable condition to initiate the geopolymerisation reaction. However, the initial setting time recorded for fly ash-based traditional geopolymer (250–480 min) [21,22], was much longer compared to the setting time measured in this study (10–55 min). The aspect of exothermic reaction must be emphasized in this case. The exothermic nature of the dissolution of the solid alkali activator creates a self-heat curing condition during the one-part mixing process, which accelerates the geopolymerisation reaction [23]. On the other hand, the traditional geopolymer uses alkali activating solution that was prepared beforehand, where the heat release was excluded in the sample preparation stage. The scenarios are illustrated in Fig. 6. The lower amount of heat release during the two-part mixing process leads to less aggressive reaction and subsequently longer initial setting time.

3.1.3. *Bulk density, water absorption and porosity*

The physical properties investigated for the OPG included the bulk density, water absorption and porosity, as shown in Fig. 7. The error bars represented the standard deviation of three samples. A clear relationship between the three properties were observed, that is the water absorption and porosity results were parallel with each other while the bulk density results demonstrated the opposite trend. Porous structures usually have larger space to contain water, besides having a lower mass per unit volume.

The bulk density increased gradually from 1954 (M1) to 2141 kg/m^3 (M3) with increasing AA/FA ratio. Further increase of this ratio showed a negligible drop of 2 kg/m^3. This suggested that the developed structures were more compact with the increasing Na_2SiO_3 dosage. The similar bulk density of M3 and M4 indicated that the addition of Na_2SiO_3 beyond the AA/

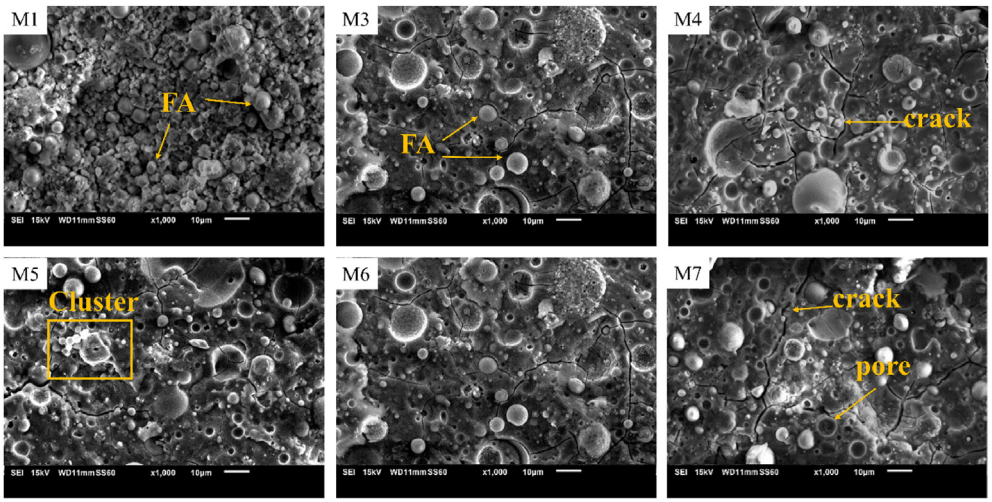

Fig. 9 – The SEM micrographs of OPG M system at 1k magnification (FA = fly ash).

FA ratio of 0.20 did not favour additional formation of dense geopolymer structure. As aforementioned, the increased Na_2SiO_3 content in the system had driven less extensive dissolution of the Na_2SiO_3 granules, which remained unreacted or partially reacted in the hardened structure. During the ageing process, the Na_2SiO_3 particles could absorb moisture from the surrounding, causing the continuous dissolution of the solid alkali activator. The geopolymerisation reaction could be progressed which potentially filled the voids with reaction products and decreased the porosity. It is noteworthy that the dissolution of Na_2SiO_3 granules occur from the outermost zone towards the inner core. If the Na_2SiO_3 particles are partially dissolved and reacted, the reaction products will form a shell around the Na_2SiO_3 particles that leave a gap between the hydrated products and the alkali particles [17], consequently contributing to air voids in the structure. The finding verifies that undissolved or partially dissolved Na_2SiO_3 particles are present in M4 which leads to increased water absorption and porosity.

Along with the increasing W/B ratio from 0.20 (M5) to 0.30 (M7), the bulk density declined by from 2193 to 2039 kg/m^3, while the water absorption and porosity increased from 3.8 to 7.8% and from 7.2 to 14.1%, respectively. The drop of bulk density and the increase of water absorption and porosity can be explained by the reduction of denser solid binder designated from the mix design and was substituted by a higher liquid content which delivered a structure with more physically bonded water. As ageing progressed, water evaporated from the matrix, subsequently creating pores or voids in the structure [24].

3.1.4. *Compressive strength*

The compressive strength of the OPGs M system after 28 days is illustrated in Fig. 8. The compressive strength was initially enhanced and then deteriorated as the AA/FA ratio increased. The compressive strength was 12.2 MPa when the AA/FA ratio was 0.10 (M1). The compressive strength increased by 687.4% (83.6 MPa) with respect to M1 when the AA/FA ratio was increased to 0.20 (M3). The massive increase in compressive strength was a result of the sufficient amount of alkali activator supplied to the mixture, which optimised the disaggregation of fly ash and promoted the formation of alkaline aluminosilicate gel. A strength reduction was observed in M4 with further increase in AA/FA ratio, corresponded to the reduced rate of reaction and increased porosity. The trend of compressive strength was supported by Dong et al. [17] for OPG mortar. The strength deterioration may also be related to the reaction product generated. It was proven previously that the Si contribution in geopolymer gel diminished with the increasing silica content [25], where the stable Si-rich phase usually contributed to a greater mechanical strength of alkali activated fly ash [26]. Hence, it was inferred that the excess anhydrous Na_2SiO_3 reduced the fraction of Si-rich gel phase, yielding a lower compressive strength. Based on the results, it is recommended that the AA/FA ratio should not be more than 0.20 in order to achieve a decent performance on fluidity and strength properties.

When the W/B ratio increased from 0.20 (M5) to 0.30 (M7), the compressive strength of the OPG increased from 62.4 to

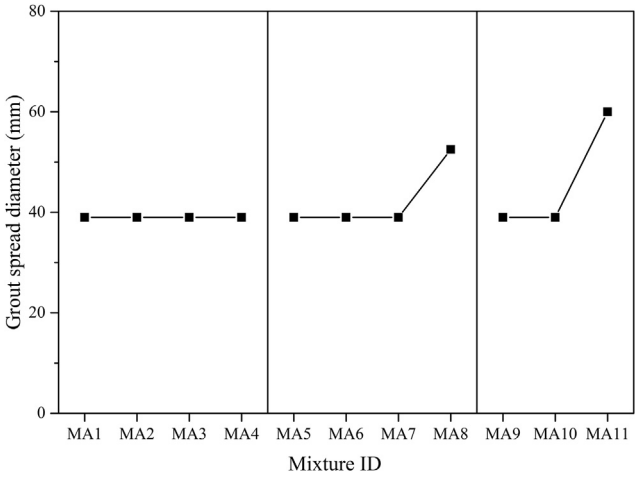

Fig. 10 – Grout spread diameter of OPG MA system.

83.6 MPa, then dropped to 28.2 MPa. As shown in Fig. 6, water was used to dissolve the solid alkali activator to enable the subsequent geopolymerisation reaction. In M5 with low W/B ratio of 0.20, water shortage led to the inefficient hydration of the solid alkali activator which prohibited the comprehensive geopolymerisation reaction. The formation of interconnecting geopolymer networks was limited and thus lowered the compressive strength. The increase of the W/B ratio from 0.20 (M5) to 0.25 (M6) enhanced the degree of polymerization of the reaction products and therefore strengthen the structure. The lower compressive strength attained by the M7 was a result of the oversupply of water in the geopolymer mixture, which lowered down the alkalinity of the mixture and discouraged the dissolution process of fly ash. In addition, high water content caused highly porous OPG structure as mentioned above, subsequently causing a strength deterioration.

In this study, M6 was selected as the optimum mixture. The AA/FA ratio of 0.20 and W/B ratio of 0.25 was proven to exhibit superior performances for Na_2SiO_3-activated OPG, as it achieved the highest 28-day compressive strength of 83.6 MPa and demonstrated decent fluidity for a wide range of applications. It should be noted that the compressive strength of this OPG was significantly higher than the OPGs developed using low calcium fly ash and Na_2SiO_3 reported in the previous literatures. For instance, the fly ash OPG mortar developed by Yang et al. [18] achieved a 28-day compressive strength of 9.5 MPa. Similarly, the OPG developed by Hajimohammadi and Deventer [25] using AA/FA of about 0.60 recorded a 21-day compressive strength of approximately 20 MPa. In order to obtain a higher compressive strength, calcium-containing raw materials, such as slag, were often incorporated [18,27]. Based on Zhou et al. [8], the OPG binder with increased substitution of fly ash by ground granulated blast furnace slag from 25 to 75% increased the 28-day compressive strength from 33 to 49 MPa. The higher compressive strength achieved by OPG synthesised in this study is because of the lower water content in this mix system and the high CaO content in the fly ash used that was able to yield calcium-containing hydrate gel, which was compact and contributed to a better mechanical properties [27]. The finding of this study suggests that Class C fly ash is viable choice for the development of OPG with excellent compressive strength without additional precursor materials required.

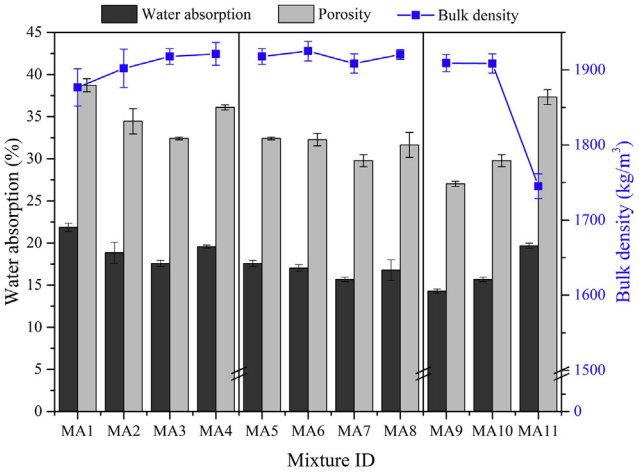

Fig. 12 – Bulk density, water absorption and porosity of OPG MA system.

3.1.5. *Microstructure analysis*

Fig. 9 depicts the SEM micrographs of the OPG M system. The spherical fly ash particles appeared thoroughly in M1 at an AA/FA ratio of 0.10. This was associated with the less promising disaggregation of fly ash particles at a low AA/FA ratio which corresponded to the relatively low compressive strength (12.2 MPa). The increase in AA/FA ratio to 0.20 (M3) and 0.25 (M4) promoted more extensive disaggregation of fly ash to develop into the bulky base, which represents the geopolymer matrix. Crack lines were observed in most of the samples. Nevertheless, broader crack lines were observed in M4 along with the interfaces of remnant fly ash particles and the geopolymer matrix, or across the partially reacted particles. The air voids developed at the outer layers of the partially reacted particles facilitated fracture formation. Therefore, the compressive strength of M4 was lower.

The varying W/B ratio contributed to minor dissimilarity in microstructures among the specimens of the M system. The

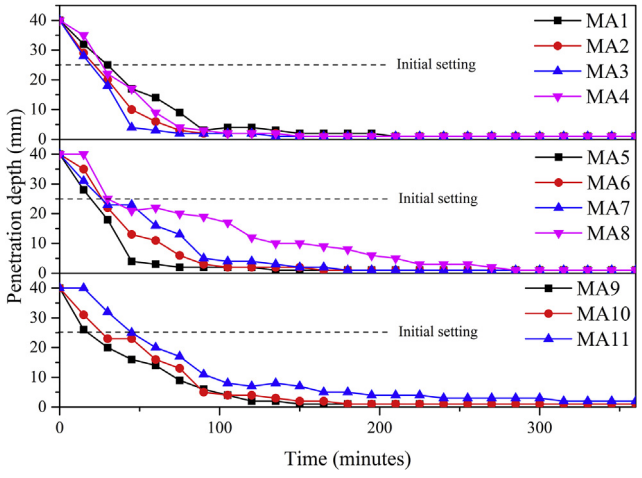

Fig. 11 – Vicat setting time of OPG MA system.

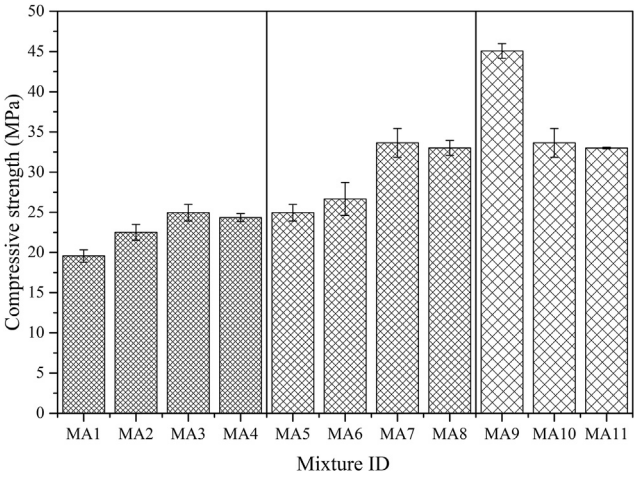

Fig. 13 – Compressive strength of MA system.

OPG with the lowest W/B ratio (M5) appeared to be more clustered, with some agglomerations of fly ash particles and reaction products on the surface. The formation of homogeneous microstructure was prohibited due to low fluidity (Fig. 4), low mobility and the restricted polycondensation reaction, as aforementioned. In addition, the low water content yielded a less effective dissolution of the anhydrous Na_2SiO_3. Although the dissolution of Na_2SiO_3 could occur along with ageing, the polycondensation of newly precipitated gel phases with the existing geopolymer matrix was unlikely. Therefore, the agglomerations of raw materials and reaction products were observed. On the other hand, increasing water promoted dissolution of raw materials as well as the transport of ions within the slurry, prompting a more homogeneous structure in M6 (W/B ratio = 0.25). However, M7 (W/B ratio = 0.30) exhibited more voids and cracks due to the high evaporation of water during ageing. The porous structure created more stress concentration points that to cause structural failure.

3.2. *One-part geopolymer with anhydrous Na_2SiO_3 and $NaAlO_2$ (MA system)*

3.2.1. *Fluidity*

The participation of $NaAlO_2$ drove the thixotropic behaviour in the OPG slurries of the MA system, where the slurries only exhibited good fluidity during mixing and vibration. Materials with thixotropic behaviour exhibit high yield stress at rest, but turns into low viscosity under applied pressure or shear force [28]. The dissolved Al from $NaAlO_2$ could attach to the Na_2SiO_3 particles, subsequently hindered the free movement of elements within the mixture, except when an external mechanical force (vibration) was exerted to disrupt the force of attraction. The observation was supported by Hajimohammadi et al. [13] whereby that proposed the soluble aluminium can reduce the solubility of silica in water because of the absorption of aqueous Al species on the surface of silica. According to Rovnaník et al. [29], the strong dipole–dipole attraction between the molecules of activators and/or precursors go against the Brownian motion, yielding thixotropic characteristic. Brownian movement is the random motion of particles suspended in a medium. When the mixing process stops and proceeds with the fluidity test under a still condition, the slurries stiffen. Therefore, most of the spread diameters remained at 39 mm (Fig. 10), regardless of the mixing compositions. Nonetheless, the thixotropic characteristic granted a decent moulding process with mild external vibration. This property suggests that the OPG is more appropriate for ex-situ applications, such as pre-cast concrete, tiles and bricks. Admixture such as superplasticizer could be added into the mixture to boost the fluidity for more diversified applications. Though this is not the intention of this study, future work on this aspect is very much encouraged.

The fluidity of the slurries from the MA system remained consistent when the AA/FA ratios were altered. The fluidity was not affected by the AA/FA ratio, but it responded to the manipulated $NaAlO_2/Na_2SiO_3$ and W/B ratio. The grout spread diameter was extended when the $NaAlO_2/Na_2SiO_3$ ratio was increased. Nevertheless, the impact was only evident when the $NaAlO_2/Na_2SiO_3$ ratio changed from 2.5 (MA7) to 3.0 (MA8). The MA7 recorded a spread diameter of 39 mm, while the MA8 recorded a spread diameter of 53 mm. The molecular mass of Na_2SiO_3 and $NaAlO_2$ were 122.1 g/mol and 82.0 g/mol, respectively. The lower molecular mass of $NaAlO_2$ indicated a lower mess degree of the compound, where the rupture of bonds was easier. As a result, the $NaAlO_2$ powder dissolved faster during the mixing process and reduced the solid fraction in the slurries when the $NaAlO_2/Na_2SiO_3$ ratio was increased, subsequently resulted in better fluidity. A similar finding was reported by Dehghani et al. [30] where a significant increment of flowability of traditional geopolymer was apprehended by increasing the Al_2O_3/SiO_2 ratio. This suggested that the fluidity value would be further extended if the $NaAlO_2/Na_2SiO_3$ ratio continued to increase.

The fluidity of the slurries was also slightly influenced by the water content. Incremental replacement of water mended the unfavourable fluidity. It was observed that the spread diameter was enlarged from 39 to 60 mm with the increased W/B ratio from 0.35 (MA9) to 0.45 (MA11). A similar observation has been reported by Oderji et al. [31]. More water was required to overcome the inter-particle friction between the solid raw materials. Although the fluidity would be further enhanced with a higher W/B ratio, it would deteriorate the mechanical strength of the OPGs, thus the approach was not encouraged.

3.2.2. *Setting time*

Fig. 11 shows the setting time of the OPG slurries of MA system over a course of 6 h. The increase of the AA/FA ratio and $NaAlO_2/Na_2SiO_3$ ratio did not significantly affect the initial setting time of the slurries. The variances of the initial setting time were in the range of 10 min for the range of AA/FA ratio and $NaAlO_2/Na_2SiO_3$ ratio studied. The initial setting time of the mixtures were in the range of 20–30 min. The results showed that increasing the AA/FA ratio from 0.10 (MA1) to 0.20 (MA3) had accelerated the initial setting time, but when the AA/FA ratio was further increased, the initial setting time was slightly reduced. When the $NaAlO_2/Na_2SiO_3$ ratio was manipulated, MA5 had the shortest initial setting time and the continuous replacement of Na_2SiO_3 by $NaAlO_2$ delayed the initial setting time. This delay was corresponded to the progressively longer final setting time, which ranged from 540 min to more than 10 h. This finding was similar to Guo et al. [32] where the final setting time of ternary one-part geopolymer increased with the increasing $NaAlO_2$ content, due to the reduction of stable network structure at the initial stage of geopolymerisation.

The fine $NaAlO_2$ powder tends to dissolve faster compared to the granular Na_2SiO_3 due to the larger surface area and lower molecular mass. However, no reduction in the setting time was observed as the $NaAlO_2/Na_2SiO_3$ ratio was increased. Firstly, the dissolution of Na_2SiO_3 granular became more difficult with the increasing amount of dissolved $NaAlO_2$ attached to the Na_2SiO_3 particles, consequently hindered the geopolymerisation reaction. The poor reaction kinetics delayed the precipitation of reaction products. Secondly, the MA slurries were rich in Al content due to the rapid dissolution of solid $NaAlO_2$ and the weaker Al–O bonds in fly ash that released alumina monomer more rapidly compared to silica monomer [33]. Concurrently, Si content was in deficit due to the poor dissolution of solid Na_2SiO_3 and the stronger Si–O

bonds in fly ash. The phenomenon hindered the formation of sialate chains because both silica and alumina were required for the formation of geopolymer sialate link. More aluminosilicate networks can only be formed after the Si was released, either from the solid Na_2SiO_3 or fly ash. Therefore, the setting time of the mixtures were extended when the $NaAlO_2/Na_2SiO_3$ ratio increased. To conclude, the increase of $NaAlO_2/Na_2SiO_3$ ratio restricted the dissolution of solid Na_2SiO_3 and delayed the precipitation of reaction products; thus, both the initial and final setting time were prolonged. Nonetheless, this finding did not serve as an indicator for the total amount of reaction products formed after 28 days, due to the potential gel formation during ageing period.

The influence of water content towards the setting time was inevitable, whereby the increase of W/B ratio led to the delay setting of OPGs, due to the prolonged condensation process. The initial setting time of OPG slurries were delayed from 15 to 45 min when the W/B ratio was increased from 0.35 (MA9) to 0.45 (MA11).

Note that a binder material with a long setting time is not favourable in contemporary construction applications. Previous research showed efforts to resolve the long setting time issue of fly ash-based traditional geopolymers. Saha and Rajasekaran [21] revealed that the initial setting time can be accelerated from ~480 to 130 min with the addition of blast furnace slag in the fly ash-based traditional geopolymer. Meanwhile, the initial setting time of the MA mixtures in the current study showed an appreciable range of 15–45 min. The result showed that $NaAlO_2$–Na_2SiO_3–activated OPG was a doable approach to overcome the long setting time of fly ash-based traditional geopolymer.

3.2.3. *Bulk density, water absorption and porosity*

The physical properties are the few key parameters for OPGs that indicate the compactness of the OPGs' structure. They are also the essential information required to support the mechanical properties of the specimens. The bulk density, water absorption and porosity of the OPG MA system are presented in Fig. 12. The bulk density increased from 1877 to 1921 kg/m^3 when the AA/FA ratio increased from 0.10 (MA1) to 0.25 (MA4). This showed that the densification of OPGs from MA1 to MA4 was affirmative. Meanwhile, the water absorption and porosity of the one-part mixes showed fluctuation. The AA/FA ratio of 0.10 was not sufficient for optimum reaction; therefore, leading to a structure with high porosity. A higher AA/FA ratio of 0.20 (MA3) led to pore refinement, due to the adequate amount of solid alkali activators that yielded a dense and compact microstructure. Further increase of AA/FA ratio yielded porous matrices. The results confirmed that the AA/FA ratio of 0.20 (MA3) was the threshold value for a compact OPG structure in the MA system. The finding was similar to the M system, and subsequently verified that the suitable solid alkali activator content for OPGs was 20% of the dry binders.

It was observed that the difference of bulk density was marginal (16.5 kg/m^3) when the $NaAlO_2/Na_2SiO_3$ ratio was manipulated. There was a slight drop in water absorption and porosity from 17.6 to 15.7% and 32.4 to 29.8%, respectively, when $NaAlO_2/Na_2SiO_3$ ratio increased from 1.5 (MA5) to 2.5 (MA7). The results revealed that the increasing $NaAlO_2$ content slightly increased the formation of reaction products that reduced the pore content of the structure. In the previous section, it was mentioned that the aqueous Al was adsorbed at the surface of granular Na_2SiO_3 during mixing. Therefore,

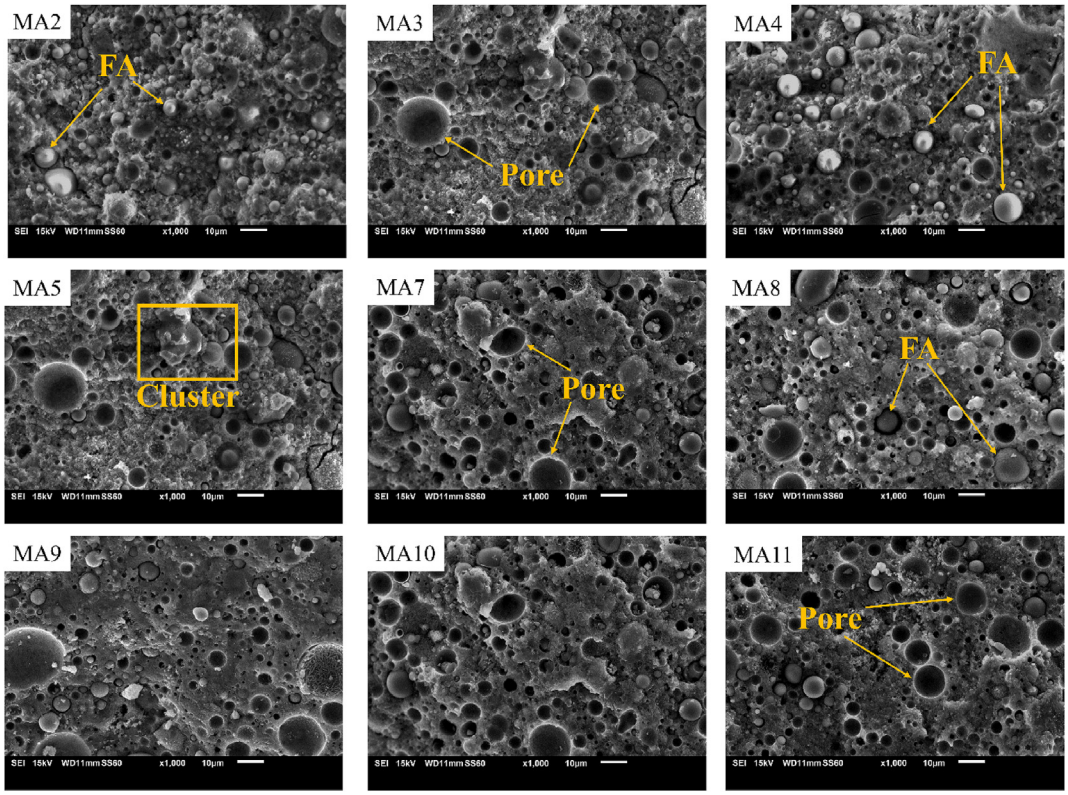

Fig. 14 – The SEM micrographs of OPG MA system at 1k magnification (FA = fly ash).

Table 3 – The ranges of properties of the OPGs.

Properties	M system	MA system
	Na_2SiO_3	$Na_2SiO_3 + NaAlO_2$
Grout spread diameter (mm)	39–183	39–60
Initial setting time (min)	10–55	15–45
Final setting time (min)	60–315	435–>600
Bulk density (kg/m^3)	1954.5–2193.3	1745.3–1925.0
Porosity (%)	7.3–20.3	27.0–38.7
Water absorption (%)	3.9–11.9	14.3–21.9
Compressive strength (MPa)	12.2–83.6	19.6–45.1

when the $NaAlO_2/Na_2SiO_3$ ratio increased, fewer aluminium ions were distracted and more Al^{3+} may have progressed with the gelation precipitations which contributed to the decreased water absorption and porosity.

The changes in W/B ratio demonstrated substantial effects on the physical properties of the OPG. The increase of W/B ratio led to a decrease in bulk density from 1909 to 1745 kg/m^3, an increase in water absorption from 14.3 to 19.7%, and porosity from 27.0 to 37.3%. These results aligned to the evaporation of water that originally resided within the structure, leaving voids during the ageing process, subsequently yielding a less dense and more porous OPG structure.

3.2.4. *Compressive strength*

Fig. 13 shows the compressive strength of the OPG MA system. When the AA/FA ratio was altered, the compressive strength varies from 19.6 to 25.0 MPa, with MA3 achieving the highest compressive strength. The MA3 mixture which comprised 20% solid alkali activator, enabled substantial geopolymerisation reaction which resulted in a stronger structure. A further increase of alkali activator content to 25% did not favour strength development due to a more porous structure generated as discussed in above. Nonetheless, the influence of the AA/FA ratio was not significant.

Interestingly, the incorporation of $NaAlO_2$ in OPG caused a strength to drop (compared to the OPGs M system), but the increased $NaAlO_2/Na_2SiO_3$ ratio from 1.5 to 2.5 slightly increased the compressive strength of the OPGs from 25.0 (MA5) to 33.7 MPa (MA7). The results suggested that the strength deterioration caused by the participation of $NaAlO_2$ in the system has its threshold value, where a continuous increase of the $NaAlO_2$ aided strength improvement to a small extent. This could be due to the increasing amount of available aluminium ions corresponding with the increasing $NaAlO_2/Na_2SiO_3$ ratio from 1.5 to 2.5. In return, the degree of reaction increased from MA5 to MA7, yielding more reaction products and increasing the compressive strength. Furthermore, it has been reported that extra Al source in raw material would increase the Si/Al atomic ratio of the geopolymer final product [34], where the compressive strength usually increases linearly with the Si/Al ratio up to a limit. Therefore, it was expected that the gel phases evolved into a higher Si/Al ratio along with the increasing $NaAlO_2/Na_2SiO_3$ ratio. The finding was in good agreement with Hajimohammadi and Deventer [25] that analysed on fly ash-based OPG, where the raw material with a lower Si/Al ratio resulted in geopolymer gel with a higher Si/Al ratio. This discussion offered a novel perspective on the distinctive effects of $NaAlO_2$ on the

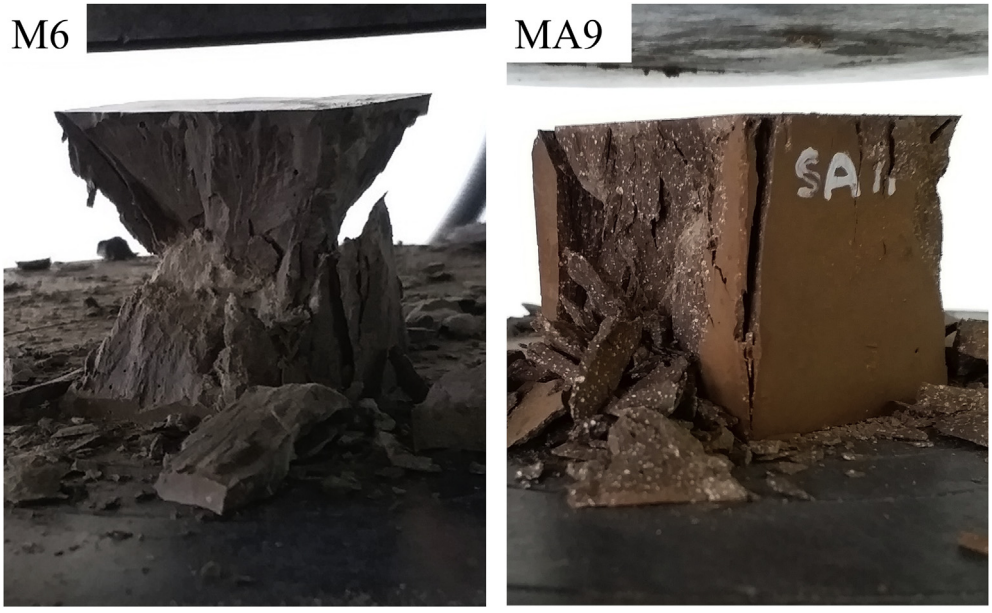

Fig. 15 – Physical observation of M6 and MA9 samples after compression test.

Table 4 – Comparison of the compressive strength performance of OPG synthesised in study and past research.

Reference	Precursor	Solid alkali activator	AA/precursor ratio	AA ratio	W/B ratio	Aggregates	Compressive strength (MPa)
This study	Class C FA	Na_2SiO_3	0.20	–	0.25	–	83.6[c]
This study	Class C FA	Na_2SiO_3, $NaAlO_2$,	0.20	2.50[a]	0.35	–	45.1[c]
Yang et al. [18]	Class F FA	Na_2SiO_3	0.49	–	0.50	Sand	9.5[c]
Mohammed et al. [27]	Class C FA	Na_2SiO_3	0.12	–	0.25	–	49.0[c]
Zhang et al. [19]	Class F FA, metakaolin	Na_2SiO_3	0.31	–	0.44	River sand	50.4[c]
Ma et al. [6]	Class F FA, GGBFS	Na_2SiO_3	0.11	–	0.35	–	58.3[c]
Zhou et al. [8]	GGBFS	Na_2SiO_3	0.11	–	0.35	Sand	56.7[c]
Hajimohammadi et al. [36]	Class F FA, geothermal silica	NaOH, $NaAlO_2$	0.48	14.36[b]	0.51	–	52.0[d]
Hajimohammadi and Deventer [12]	Rice Husk Ash	$NaAlO_2$	0.35	–	0.45	–	22.0[d]

Note:
[a] $NaAlO_2/Na_2SiO_3$ ratio.
[b] $NaAlO_2$/NaOH ratio.
[c] Compressive strength after 28 days.
[d] Compressive strength after 21 days.

evolution of the Si/Al ratio in reaction products. Future research may extend this work by determining the threshold value of the $NaAlO_2/Na_2SiO_3$ ratio that breakeven the strength drop.

The increase of W/B ratio adversely affected the compressive strength The compressive strength dropped from 45.1 to 33.0 MPa when the W/B ratio increased from 0.35 (MA9) to 0.45 (MA11). The result was in line with the physical analysis obtained. The bulk density was reduced; the water absorption and porosity were increased. An increase in water diluted the alkalinity of the one-part mixtures, but the disaggregation of fly ash required high alkalinity conditions. As a result, geopolymerisation reaction was discouraged when the W/B ratio was increased, subsequently the compressive strength was reduced.

Despite the low fluidity, the optimum mix design appointed from this geopolymer system was MA9. A mixture with better fluidity could be selected, but the mixtures only displayed a small improvement in fluidity in exchange for a significant strength loss. The MA9 attained a compressive strength of 45.1 MPa, which was higher than the required 28-day compressive strength for all types of hydraulic cement specified in ASTM C1157 (>28 MPa), and masonry grout as specified in ASTM C476 (>14 MPa). The compressive strength of MA9 also surpassed the 3 weeks compressive strength of $NaAlO_2$-activated rice husk ash OPG (22 MPa) [12], and the traditional geopolymer fabricated from silica fume, $NaAlO_2$ and NaOH (26 MPa) [35].

3.2.5. *Microstructure analysis*

The SEM micrographs of the OPG MA system are displayed in Fig. 14. The dark circular indentations represent pores or voids, whereas the bright circular convex items represent the fly ash particles. Generally, the OPGs consisted of a substantial amount of pores and voids caused by the escape of physically bonded water from the structure during ageing process. Clear traces of spherical fly ash particles were visible throughout the SEM images, suggesting a lower level of geopolymerisation reaction. Nonetheless, reaction products were developed as the friable base structure, which signified the development of an amorphous geopolymer matrix.

As shown in Fig. 14, the increase of the AA/FA ratio exerted minor changes between the mixtures. The microstructures contained pores, unreacted fly ash particles, and friable bases. A closer inspection showed that at AA/FA ratio of 0.15 (MA2), a larger amount of fly ash particles was retained in the structure when compared to MA3 and MA4 with AA/FA ratios of 0.20 and 0.25, respectively. This indicates that the MA2 experienced a less effective fly ash disaggregation when compared to MA3 and MA4. The observation was corresponded to the lower 28-day compressive strength achieved by MA2 (22.5 MPa). Nonetheless, MA3 suffered from raw material agglomeration with a cluster of fly ash particles visible from the micrograph. This seemed reasonable considering the poor fluidity character of this mix design, as shown in Fig. 10.

Meanwhile, an increase in the $NaAlO_2/Na_2SiO_3$ ratio beyond 1.5 was able to overcome the agglomeration of particles. The increase replacement of Na_2SiO_3 by $NaAlO_2$ resulted in a homogeneous and smooth microstructure with the fly ash particles scattered more evenly. This justified that the dispersion of elements was less constrained, subsequently caused better polycondensation reaction. The enhancement was attributed from the better fluidity experienced by the OPG slurries when the $NaAlO_2/Na_2SiO_3$ ratio was increased (Fig. 10). In addition, a larger portion of the dense geopolymer matrix was visible in MA7 and MA8 when compared to MA5. The findings advanced the understanding that treating $NaAlO_2$ as the primary alkali activator for a fly ash-based OPG could significantly encourage microstructural development.

Another observation from the SEM micrograph showed that the lower W/B ratio of 0.35 (MA9) resulted in a specimen with a more compact base, compared to OPGs with higher W/B ratios (MA10 and MA11). Note that the smooth and homogeneous base indicated a greater portion of gel phases. Increasing water content led to incompact structure, which was consistent with the increasing porosity along with the increasing W/B ratio (Fig. 12). Even though a less porous structure had higher strength and was more durable, the mix

design with a higher W/B ratio exhibited better fluidity that was more favourable for the fabrication process. The mix design could be manipulated accordingly to suit the applications. For example, a less porous OPG could be practised in corrosive conditions owing to the low permeability which could reduce the structural deterioration. Likewise, OPG with better fluidity and relatively low compressive strength could be applied in grout for masonry and self-compacting concrete.

3.3. *Varying solid activators: role and binding phase*

The comparison of fresh and hardened properties of OPG activated with varying solid activators are summarized in Table 3. Geopolymer mixture with Na_2SiO_3 had a better fluidity, whereas geopolymer mixture with the replacement of $NaAlO_2$ as solid activator had a thixotropic rheological behaviour. Thus, the one-part geopolymer mixture with $NaAlO_2$ and Na_2SiO_3 (MA system) requires a higher W/B ratio (W/B ratio of 0.30–0.45) than that activated with only Na_2SiO_3 (M system) (W/B ratio of 0.20–0.30) to allow better distribution of particles and formation of interconnected geopolymer networks. However, the higher water content in the MA system may reduce the alkalinity of mixtures, producing a greater amount of pores and lower compressive strength. Therefore, highly porous microstructures were revealed in the OPG MA system (Fig. 14) compared to those of the M system (Fig. 9).

Even with a higher water content, the MA system mixture had a short initial setting time. The short setting time was due to the finer $NaAlO_2$ activator which can dissolve quicker than the granular Na_2SiO_3, subsequently allowing an earlier initiation of geopolymerisation reaction. It is noted that the fineness of the solid alkali activators is important. However, the final setting time of the MA system was much longer than the M system, implying the lower rate of reaction due to the delayed dissolution of Si from the interaction between the $NaAlO_2$ and Na_2SiO_3. As mentioned before, $NaAlO_2$ will hinder the effective dissolution of Na_2SiO_3. The statement was proven in Fig. 15, whereby small white dots of Na_2SiO_3 remnants were seen scattered in the MA samples activated with $NaAlO_2$ and Na_2SiO_3. No white dot was visible in the M samples activated with only Na_2SiO_3. Regardless, the white dots would progressively react with moisture from the surrounding, subsequently disappearing after a longer ageing time.

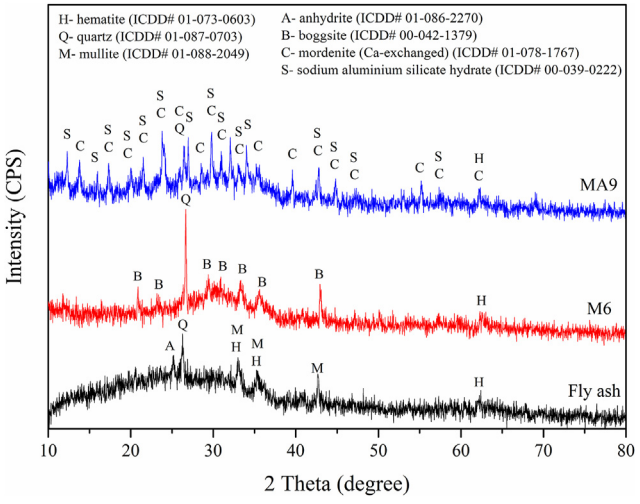

Fig. 16 – The XRD diffractograms of fly ash, M6 and MA9.

To summarise, the unique chemistry of $NaAlO_2$ and Na_2SiO_3 drove varying properties between the OPGs from both M and MA system. For the OPG M system, the dissolved Na_2SiO_3 created a sufficiently high pH condition to initiate the fly ash disaggregation, where silicate and aluminate species can be generated instantly. Meanwhile, for the OPG MA system, the dissolved $NaAlO_2$ species mingled with the Na_2SiO_3 and fly ash particles. The inclusion of $NaAlO_2$ led to additional interaction with the undissolved Na_2SiO_3 that hindered the instantaneous disaggregation of fly ash and thus the release of silicate and aluminate species occurred at a different pace. The reactions yielded distinctive properties of the OPGs. Eventually, both systems successfully produced feasible binder materials for building and construction purposes.

Table 4 summarises the compressive strength performance of OPG compared to those reported by other researchers. The OPG activated using anhydrous Na_2SiO_3 synthesised in this study exhibited higher compressive strength compared to those reported in past literature. For instance, Yang et al. [18] reported compressive strength of merely 9.5 MPa for OPG mortar synthesised with Class F fly ash and Na_2SiO_3. The lower compressive strength was most probably due to the low calcium content of the Class F fly ash and higher water content. The current study demonstrated a higher compressive strength than the OPG prepared by Mohammed et al. [27], despite using the same W/B ratio and same type of fly ash (i.e., Class C fly ash). The higher compressive strength obtained in this study was due to a higher AA/FA ratio with additional vibrating step during the mixing process. Greater amount of solid activators led to greater amount of Si and Al species to participate in the geopolymerisation reaction. Besides, it was found out that the OPG incorporated with metakaolin required a higher amount of Na_2SiO_3, whereas OPG involving ground granulated blast furnace slag (GGBFS) required a lower amount of Na_2SiO_3 in order to achieve a similar compressive strength.

The compressive strength of OPG activated with Na_2SiO_3 and $NaAlO_2$ in this study was higher than that produced by Hajimohammadi and Deventer [12] but lower than that produced by Hajimohammadi et al. [36]. In comparison with previous studies, the OPG mix design in this study used the lowest amount of solid activator (AA/precursor ratio of 0.20) and water (W/B ratio of 0.35). Hajimohammadi et al. [36] used fly ash and geothermal silica as precursor, NaOH and $NaAlO_2$ as activators. An additional 240% solid activators (AA/precursor ratio of 0.48) yielded an OPG with a compressive strength of 52.0 MPa, which is 15.3% higher than the OPG of this study. The outcome was not rewarding considering that high amount of solid activator was used. Besides that, geothermal silica was known to contribute higher strength owing to the extra silicate supplied. Thus, a slightly higher compressive strength was obtained. Hajimohammadi and Deventer [12] utilised rice husk ash as precursor and sole $NaAlO_2$ as solid activator, a modest strength of 22 MPa was obtained after 3 weeks even though a higher $NaAlO_2$ content (AA/precursor ratio of 0.35) was used. These data infer that a

mix design using Class C fly ash with low solid activator content is able to yield OPG with a decent strength performance, compared to other precursor materials.

3.3.1. *Phase identification*

Fig. 16 demonstrates the XRD diffractograms of fly ash, M6 and MA9. The differences of these XRD patterns significantly verified the formation of different gel phases in the OPGs with varying alkali activators. The primary minerals found in fly ash were hematite (ICDD# 01-073-0603), quartz (ICDD# 01-087-0703) and mullite (ICDD# 01-088-2049). The fly ash also showed a trace amount of anhydrite (ICDD# 01-086-2270) at 25° 2θ. A broad hump could be observed from the XRD spectrum of fly ash registered from 10° to 40° 2θ. The halo in the spectrum was resulted from the diffuse scattering of the amorphous structure in the materials [37], hence verifying its vitreous characteristic.

The hump was also present in OPGs, but it was narrower and shifted to higher degrees ($2\theta = 25°–40°$). This indicated that the disaggregation of amorphous phases of fly ash took place and yielded new amorphous phases in OPGs [37]. Besides, hematite and quartz peaks appeared at all the diffractograms of the OPG regardless of the types of alkali activators incorporated. This meant that hematite and quartz did not fully partake in the reaction. The finding was in good agreement with the SEM images in Figs. 9 and 14, whereby the fly ash particles could be found in the OPG structure.

The M6 mainly consisted of boggsite (ICDD# 00-042-1379). Boggsite is an orthorhombic mineral, with the compound name of sodium calcium aluminium silicate hydrate designated (N,C)-A-S-H. For geopolymer developed using Class F fly ash, the N-A-S-H gel was typically formed due to the lack of CaO content. But pure N-A-S-H gel was unlikely to dominate the gel phase in a calcium-containing system [38]. In a Ca-rich system, Na_2O, CaO, Al_2O_3, SiO_2 and H_2O were involved in the geopolymerisation reaction. In the OPG M system, the dissolution of solid Na_2SiO_3 and disaggregation of fly ash released a high concentration of Na, Ca, Al and Si at the early stage of mixing, where all of the elements can be precipitated simultaneously. Concurrently, the self-heat curing condition occurred, caused the accelerated condensation reaction, whereby the time given for the ion exchange in the systems was limited. Thus, both Na^+ and Ca^{2+} ions acted as the charge balancer in the tetrahedral SiO_4 and AlO_4 linked chain structure. Eventually, the 3D (N,C)-A-S-H gel was generated.

Unlike M6, distinct N-A-S-H and C-A-S-H gel were detected in MA9, as shown by the presence of mordenite (Ca-exchanged) (ICDD# 01-078-1767) and sodium aluminium silicate hydrate (ICDD# 00-039-0222). Mordenite (Ca-exchanged) is the mineral name of the compound C-A-S-H. The analysis confirmed the coexistence of N-A-S-H and C-A-S-H gels in the OPG product. These diffraction peaks were usually found in geopolymer produced from slag and fly ash blends [39,40]. The OPG MA system experienced delayed precipitation due to the poor interaction between the solid alkali activators and the low Si content at the early stage of mixing. Therefore, the ion exchange was prolonged during the setting period, allowing sufficient time for the formation of distinctive N-A-S-H and C-A-S-H gel. The (N,C)-A-S-H gel may be generated at the initial stage of mixing, but it was unstable in the presence of Ca. This was because the C-A-S-H gel formation was more encouraged as Ca^{2+} ions have stronger polarizing power than Na^+ ions [41]. Therefore, the Ca^{2+} ions were took in by the reaction product to transform the (N,C)-A-S-H gel to a C-A-S-H gel. The scenario did not occur in the OPG M system due to the limited time for extensive ion exchange. The Ca^{2+} ions were gradually exhausted at the later stage of setting for the OPG MA system. When limited Ca^{2+} was available for polymerization of silicate and aluminate, N-A-S-H gel precipitated. As mentioned by Chindaprasirt et al. [42] the N-A-S-H gel was the secondary reaction product in the high-calcium fly ash-based traditional geopolymer prepared using a two-part mixing method.

The findings revealed that the types of gelation phases were different when different types of solid alkali activators were involved. The primary factor for the difference was the ions concentration in the system throughout the setting period. As referring to microstructure of the aged OPGs (Fig. 9), the (N,C)-A-S-H gel exhibited a smooth and dense matrix, giving the sample a stronger structure. On the other hand, the coexistence of N-A-S-H and C-A-S-H binding phases were less space-filling as can be proven from the friable microstructures (Fig. 14), leading to a weaker structure. The (N,C)-A-S-H gel prompted a higher compressive strength of the M system when compared to the MA system with coexisting N-A-S-H and C-A-S-H gel phases. The observation was consistent with the finding of Ismail et al. [43] which stated that the N-C-A-S-H gel exhibited smaller pores and a higher degree of crosslinking than the C-A-S-H gel type.

3.3.2. *Functional group identification*

The functional group identification was conducted on the fly ash and the optimum OPGs to ensure the evolution of raw material into a geopolymer compound. The FTIR spectra of fly ash and the optimum OPGs were shown in Fig. 17. From the spectra, it was found out that the absorption bands of fly ash are similar to that of M6 and MA9. The absorption bands in the region of 3300–3500 cm^{-1} were due to the asymmetric and symmetric stretching vibrations of the –OH group, while the absorption bands at around 1600 cm^{-1} were caused by the bending vibrations of H–O–H [44]. The presence of these bands in fly ash were associated with the absorbed moisture.

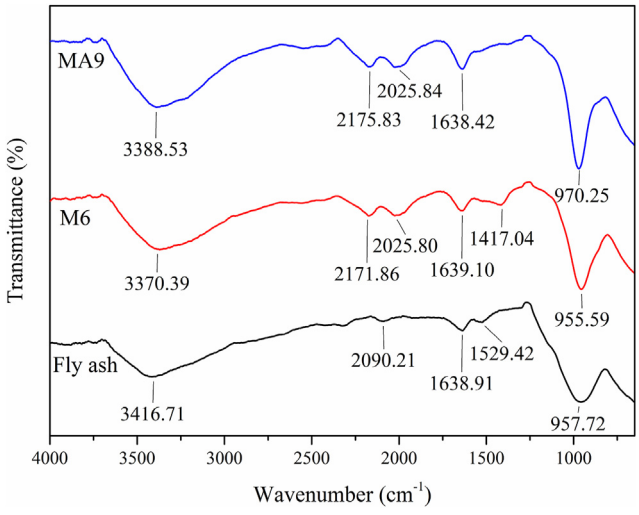

Fig. 17 – The FTIR spectra of fly ash, M6 and MA9.

For OPGs samples, these bands were due to the water molecules entrapped in the cavities of the geopolymeric framework. The insignificant absorption band located at the ranges of 2200–2000 cm^{-1} and 1530–1400 cm^{-1} were due to the O–C–O stretching vibrations [44,45]. The carbonate remained in the fly ash during the process of coal-burning led to the presence of these bands in fly ash. Meanwhile, the diffusion of atmospheric carbonate into the OPG samples during the ageing process caused the development of the absorption band.

For the raw fly ash, the band at 958 cm^{-1} was caused by the asymmetric stretching vibrations of Si–O–T (T = Si or Al) [10]. The wide and intense bands at this region justified that the fly ash comprised the amorphous phase (Si–O and Al–O groups), quartz and mullite [46]. This band was also a typical assignment for silicate-activated OPG [10,11]. Other than signifying the main geopolymer bonds (Si–O–Si and Si–O–Al), Criado et al. [46] discovered that these bands were the outcome of the overlapping bands generated by the unreacted fly ash, quartz and mullite. The observation can be ascertained from the XRD pattern as shown in Fig. 17. For M6 and MA9, the absorption bands shifted from 958 cm^{-1} to 956 cm^{-1} and 970 cm^{-1}, respectively. These bands in OPGs were associated with the amorphous aluminosilicate gel phase developed.

4. Conclusion

In this article, the fresh and hardened properties of Class C fly ash-based OPG with single and binary solid alkali activators were investigated. Two conclusions were drawn based on the test result.

1. For OPG developed via single alkali activator, which was entirely by anhydrous Na_2SiO_3, the slurries exhibited excellent fluidity. The initial setting time ranged from 10 to 55 min while the final setting time ranged from 60 min to 315 min. The optimum mixture with AA/FA ratio of 0.20 and W/B ratio of 0.25 recorded the highest compressive strength of 83.6 MPa. The optimum Na_2SiO_3-activated OPG displayed a large portion of dense matrix, which was identified as the (N,C)-A-S-H gel phase. The findings advocated that a high strength geopolymer was viable through the "just add water" approach with Class C fly ash and anhydrous Na_2SiO_3.
2. For OPG developed from binary alkali activator, which was by the combination of solid $NaAlO_2$ and Na_2SiO_3, the slurries exhibited thixotropic behaviour. The initial setting time ranged from 20 min to 45 min but exhibited extended final setting time (from 435 min to more than 10 h). Due low efficiency reaction, the developed geopolymer gel was friable, subsequently resulted in moderate compressive strength. The optimum OPG was produced with an AA/FA ratio of 0.20, $NaAlO_2/Na_2SiO_3$ of 2.50 and W/B ratio of 0.35, attained a compressive strength of 45.1 MPa. The geopolymer matrix consisted of the coexistence of N-A-S-H and C-A-S-H.

A comparison study was also carried out between the two OPGs synthesized. Generally, it was confirmed that the performances of OPG incorporated with solid $NaAlO_2$ were more modest in the aspect of fluidity and compressive strength compared to that of the Na_2SiO_3-activated OPG. Nonetheless, the OPG MA system are still adequate to be used in construction applications. In addition, the more environmentally friendly production process and the lower cost of solid $NaAlO_2$ is more worthwhile to fabricate OPG for lower strength purposes instead of anhydrous Na_2SiO_3. The results of both systems of OPG also advanced the understanding that the addition of $NaAlO_2$ in OPG does not yield linearly decreasing compressive strength. Furthermore, the incorporation of $NaAlO_2$ caused the strength reduction by obstructing the dissolution of Na_2SiO_3, but the continuous supply of $NaAlO_2$ in the OPG MA system is capable to restore the compressive strength to a small extent due to the increasing involvement of $NaAlO_2$ in the reaction. Taken together, this offers a novel perspective on the effect of $NaAlO_2$ replacement in Na_2SiO_3-activated fly ash-based OPG on mechanical strength development.

Declaration of Competing Interest

The authors declare that they have no known competing financial interests or personal relationships that could have appeared to influence the work reported in this paper.

Acknowledgements

This work was supported by Fundamental Research Grant Scheme (FRGS/1/2020/TK01/UNIMAP/02/2) from the Ministry of Higher Education Malaysia.

REFERENCES

[1] Luukkonen T, Abdollahnejad Z, Yliniemi J, Kinnunen P, Illikainen M. One-part alkali-activated materials: a review. Cement Concr Res 2018;103:21–34. https://doi.org/10.1016/j.cemconres.2017.10.001.
[2] Andrew RM. Global CO_2 emissions from cement production. Earth Syst Sci Data 2018;10(1):195–217. https://doi.org/10.5194/essd-10-195-2018.
[3] Davidovits J. Geopolymers and geopolymeric materials. J Therm Anal Calorim 1989;35(2):429–41. https://doi.org/10.1007/BF01904446.
[4] De Weerdt K. Geopolymers—state of the art, COIN Project Report 37. 2011.
[5] Matalkah F, Xu L, Wu W, Soroushian P. Mechanochemical synthesis of one-part alkali aluminosilicate hydraulic cement. Mater Struct 2017;50(1):97. https://doi.org/10.1617/s11527-016-0968-4.
[6] Ma C, Long G, Shi Y, Xie Y. Preparation of cleaner one-part geopolymer by investigating different types of commercial sodium metasilicate in China. J Clean Prod 2018;201:636–47. https://doi.org/10.1016/j.jclepro.2018.08.060.
[7] Oderji SY, Chen B, Ahmad MR, Shah SFA. Fresh and hardened properties of one-part fly ash-based geopolymer binders cured at room temperature: effect of slag and alkali activators. J Clean Prod 2019;225:1–10. https://doi.org/10.1016/j.jclepro.2019.03.290.

[8] Zhou S, Ma C, Long G, Xie Y. A novel non-Portland cementitious material: mechanical properties, durability and characterization. Constr Build Mater 2020;238:117671. https://doi.org/10.1016/j.conbuildmat.2019.117671.
[9] Ma C, Zhao B, Guo S, Long G, Xie Y. Properties and characterization of green one-part geopolymer activated by composite activators. J Clean Prod 2019;220:188–99. https://doi.org/10.1016/j.jclepro.2019.02.159.
[10] Askarian M, Tao Z, Samali B, Adam G, Shuaibu R. Mix composition and characterisation of one-part geopolymers with different activators. Constr Build Mater 2019;225:526–37. https://doi.org/10.1016/j.conbuildmat.2019.07.083.
[11] Mohammed BS, Haruna S, Wahab M, Liew M, Haruna A. Mechanical and microstructural properties of high calcium fly ash one-part geopolymer cement made with granular activator. Heliyon 2019;5(9):2255. https://doi.org/10.1016/j.heliyon.2019.e02255.
[12] Hajimohammadi A, van Deventer JS. Solid reactant-based geopolymers from rice hull ash and sodium aluminate. Waste Biomass Valorization 2017;8(6):2131–40. https://doi.org/10.1007/s12649-016-9735-6.
[13] Hajimohammadi A, Provis JL, Van Deventer JS. One-part geopolymer mixes from geothermal silica and sodium aluminate. Ind Eng Chem Res 2008;47(23):9396–405. https://doi.org/10.1021/ie8006825.
[14] Sturm P, Gluth G, Brouwers H, Kühne H-C. Synthesizing one-part geopolymers from rice husk ash. Constr Build Mater 2016;124:961–6. https://doi.org/10.1016/j.conbuildmat.2016.08.017.
[15] Sturm P, Greiser S, Gluth G, Jäger C, Brouwers H. Degree of reaction and phase content of silica-based one-part geopolymers investigated using chemical and NMR spectroscopic methods. J Mater Sci 2015;50(20):6768–78. https://doi.org/10.1007/s10853-015-9232-5.
[16] Sturm P, Gluth G, Simon S, Brouwers H, Kühne H-C. The effect of heat treatment on the mechanical and structural properties of one-part geopolymer-zeolite composites. Thermochim Acta 2016;635:41–58. https://doi.org/10.1016/j.tca.2016.04.015.
[17] Dong M, Elchalakani M, Karrech A. Development of high strength one-part geopolymer mortar using sodium metasilicate. Constr Build Mater 2020;236:117611. https://doi.org/10.1016/j.conbuildmat.2019.117611.
[18] Yang K-H, Song J-K, Ashour AF, Lee E-T. Properties of cementless mortars activated by sodium silicate. Constr Build Mater 2008;22(9):1981–9. https://doi.org/10.1016/j.conbuildmat.2007.07.003.
[19] Zhang H-Y, Liu J-C, Wu B. Mechanical properties and reaction mechanism of one-part geopolymer mortars. Constr Build Mater 2021;273:121973. https://doi.org/10.1016/j.conbuildmat.2020.121973.
[20] Ranjbar N, Kuenzel C, Spangenberg J, Mehrali M. Hardening evolution of geopolymers from setting to equilibrium: a review. Cement Concr Compos 2020;114:103729. https://doi.org/10.1016/j.cemconcomp.2020.103729.
[21] Saha S, Rajasekaran C. Enhancement of the properties of fly ash based geopolymer paste by incorporating ground granulated blast furnace slag. Constr Build Mater 2017;146:615–20. https://doi.org/10.1016/j.conbuildmat.2017.04.139.
[22] Kuri JC, Khan MNN, Sarker PK. Fresh and hardened properties of geopolymer binder using ground high magnesium ferronickel slag with fly ash. Constr Build Mater 2021;272:121877. https://doi.org/10.1016/j.conbuildmat.2020.121877.
[23] Suwan T, Fan M. Effect of manufacturing process on the mechanisms and mechanical properties of fly ash-based geopolymer in ambient curing temperature. Mater Manuf Process 2017;32(5):461–7. https://doi.org/10.1080/10426914.2016.1198013.
[24] Duxson P, Fernández-Jiménez A, Provis JL, Lukey GC, Palomo A, van Deventer JS. Geopolymer technology: the current state of the art. J Mater Sci 2007;42(9):2917–33. https://doi.org/10.1007/s10853-006-0637-z.
[25] Hajimohammadi A, van Deventer JS. Characterisation of one-part geopolymer binders made from fly ash. Waste Biomass Valorization 2017;8(1):225–33. https://doi.org/10.1007/s12649-016-9582-5.
[26] Fernández-Jiménez A, Palomo A, Sobrados I, Sanz J. The role played by the reactive alumina content in the alkaline activation of fly ashes. Microporous Mesoporous Mater 2006;91(1–3):111–9. https://doi.org/10.1016/j.micromeso.2005.11.015.
[27] Mohammed BS, Haruna S, Liew M. Optimization and characterization of cast in-situ alkali-activated pastes by response surface methodology. Constr Build Mater 2019;225:776–87. https://doi.org/10.1016/j.conbuildmat.2019.07.267.
[28] Panda B, Tan MJ. Experimental study on mix proportion and fresh properties of fly ash based geopolymer for 3D concrete printing. Ceram Int 2018;44(9):10258–65. https://doi.org/10.1016/j.ceramint.2018.03.031.
[29] Rovnaník P, Rovnaníková P, Vyšvařil M, Grzeszczyk S, Janowska-Renkas E. Rheological properties and microstructure of binary waste red brick powder/metakaolin geopolymer. Constr Build Mater 2018;188:924–33. https://doi.org/10.1016/j.conbuildmat.2018.08.150.
[30] Dehghani A, Aslani F, Panah NG. Effects of initial SiO_2/Al_2O_3 molar ratio and slag on fly ash-based ambient cured geopolymer properties. Constr Build Mater 2021;293:123527. https://doi.org/10.1016/j.conbuildmat.2021.123527.
[31] Oderji SY, Chen B, Shakya C, Ahmad MR, Shah SFA. Influence of superplasticizers and retarders on the workability and strength of one-part alkali-activated fly ash/slag binders cured at room temperature. Constr Build Mater 2019;229:116891. https://doi.org/10.1016/j.conbuildmat.2019.116891.
[32] Guo S, Ma C, Long G, Xie Y. Cleaner one-part geopolymer prepared by introducing fly ash sinking spherical beads: properties and geopolymerization mechanism. J Clean Prod 2019;219:686–97. https://doi.org/10.1016/j.jclepro.2019.02.116.
[33] Palomo Á, Kavalerova E, Fernández-Jiménez A, Krivenko P, García-Lodeiro I, Maltseva O. A review on alkaline activation: new analytical perspectives. 2015. https://doi.org/10.3989/mc.2014.00314.
[34] Oh JE, Moon J, Oh S-G, Clark SM, Monteiro PJ. Microstructural and compositional change of NaOH-activated high calcium fly ash by incorporating Na-aluminate and co-existence of geopolymeric gel and C–S–H (I). Cement Concr Res 2012;42(5):673–85. https://doi.org/10.1016/j.cemconres.2012.02.002.
[35] Brew D, MacKenzie K. Geopolymer synthesis using silica fume and sodium aluminate. J Mater Sci 2007;42(11):3990–3. https://doi.org/10.1007/s10853-006-0376-1.
[36] Hajimohammadi A, Provis JL, Van Deventer JS. Effect of alumina release rate on the mechanism of geopolymer gel formation. Chem Mater 2010;22(18):5199–208.
[37] Singh GB, Subramaniam KV. Quantitative XRD study of amorphous phase in alkali activated low calcium siliceous fly

ash. Constr Build Mater 2016;124:139–47. https://doi.org/10.1016/j.conbuildmat.2016.07.081.

[38] Garcia-Lodeiro I, Donatello S, Fernández-Jiménez A, Palomo Á. Hydration of hybrid alkaline cement containing a very large proportion of fly ash: a descriptive model. Materials 2016;9(7):605. https://doi.org/10.3390/ma9070605.

[39] Rafeet A, Vinai R, Soutsos M, Sha W. Effects of slag substitution on physical and mechanical properties of fly ash-based alkali activated binders (AABs). Cement Concr Res 2019;122:118–35. https://doi.org/10.1016/j.cemconres.2019.05.003.

[40] Ramagiri KK, Kar A. Effect of high-temperature on the microstructure of alkali-activated binder. Mater Today Proc 2020;28:1123–9. https://doi.org/10.1016/j.matpr.2020.01.093.

[41] Garcia-Lodeiro I, Palomo A, Fernández-Jiménez A, Macphee D. Compatibility studies between NASH and CASH gels. Study in the ternary diagram Na2O–CaO–Al2O3–SiO2–H2O. Cement Concr Res 2011;41(9):923–31. https://doi.org/10.1016/j.cemconres.2011.05.006.

[42] Chindaprasirt P, De Silva P, Sagoe-Crentsil K, Hanjitsuwan S. Effect of SiO_2 and Al_2O_3 on the setting and hardening of high calcium fly ash-based geopolymer systems. J Mater Sci 2012;47(12):4876–83. https://doi.org/10.1007/s10853-012-6353-y.

[43] Ismail I, Bernal SA, Provis JL, San Nicolas R, Hamdan S, van Deventer JS. Modification of phase evolution in alkali-activated blast furnace slag by the incorporation of fly ash. Cement Concr Compos 2014;45:125–35. https://doi.org/10.1016/j.cemconcomp.2013.09.006.

[44] Panias D, Giannopoulou IP, Perraki T. Effect of synthesis parameters on the mechanical properties of fly ash-based geopolymers. Colloid Surf A Physicochem Eng Asp 2007;301(1–3):246–54. https://doi.org/10.1016/j.colsurfa.2006.12.064.

[45] Bouaissi A, Li L-y, Abdullah MMAB, Bui Q-B. Mechanical properties and microstructure analysis of FA-GGBS-HMNS based geopolymer concrete. Constr Build Mater 2019;210:198–209. https://doi.org/10.1016/j.conbuildmat.2019.03.202.

[46] Criado M, Fernández-Jiménez A, Palomo A. Alkali activation of fly ash: effect of the SiO_2/Na_2O ratio: Part I: FTIR study. Microporous Mesoporous Mater 2007;106(1–3):180–91. https://doi.org/10.1016/j.micromeso.2007.02.055.